

SLINGATRON OVERVIEW

D.A.Tidman
Slingatron Technologies Inc,
6801 Benjamin Street, McLean, VA 22101
January 6, 2006

Nomenclature

D = projectile diameter
 ΔV = projectile velocity gain per turn
 ΔR = gap between spiral turns
 f = gyration frequency
 $g_v = v^2 / r$ = centripetal acceleration
 g_E = earth's gravity acceleration
 L = projectile length
 $m = (\pi / 4) \rho_{proj} L D^2$ = cylindrical projectile mass
 M_{system} = slingatron system mass
 μ = projectile sliding friction coefficient
 P = bearing gas pressure
 θ = angle between projectile V and gyration v .
 r = radius of gyration motion
 R = radius of curvature of slingatron track
 ρ_{proj} = density of projectile
 t = time
 v = gyration speed of slingatron
 V = projectile speed

1.1 Introduction

In this chapter we give an overview of the slingatron mass accelerator concept, and make use of a few approximate equations to support the discussion. More exact equations for the dynamics together with computer models are given in chapter 2 and in the publications¹⁻¹⁵ listed in the Appendices. The important role of the projectile gas bearing friction coefficient and its theoretical decrease with increasing projectile size is discussed in Chapter 3. Some specific mechanical design approaches for these machines are then described in Chapter 4, from which it also becomes evident that the slingatron scales well to very large-scale machines capable of accelerating massive projectiles. Finally, a few potential applications are briefly discussed in chapter 5.

In a slingatron, projectiles are accelerated along a rigid tube that typically has circular or spiral turns, or combinations of these geometries in two or three dimensions. A projectile is accelerated in the curved tube by propelling the entire tube in a small-amplitude circular orbit of constant frequency without changing the orientation of the tube, i.e., the entire tube gyrates but does not spin. This gyration continually displaces the tube with a component along the direction of the centripetal force acting on the projectile, so that work is continually done on the projectile as it advances through the machine. The centripetal force experienced by the projectile is the accelerating force, and is proportional to the projectile mass.

1.2 Classical Slings

We start by recalling the classical sling, for which two versions are shown in Figures 1(a) and 1(b). Figure 1(a) shows a sling in which a mass is whirled around a circle of constant radius R with an *increasing frequency* that results in increasing speed for the mass m . Figure 1(b) shows a variation of a classical sling in which the string has a swing radius R that continually increases in length at a rate \dot{R} so that the projectile moves out

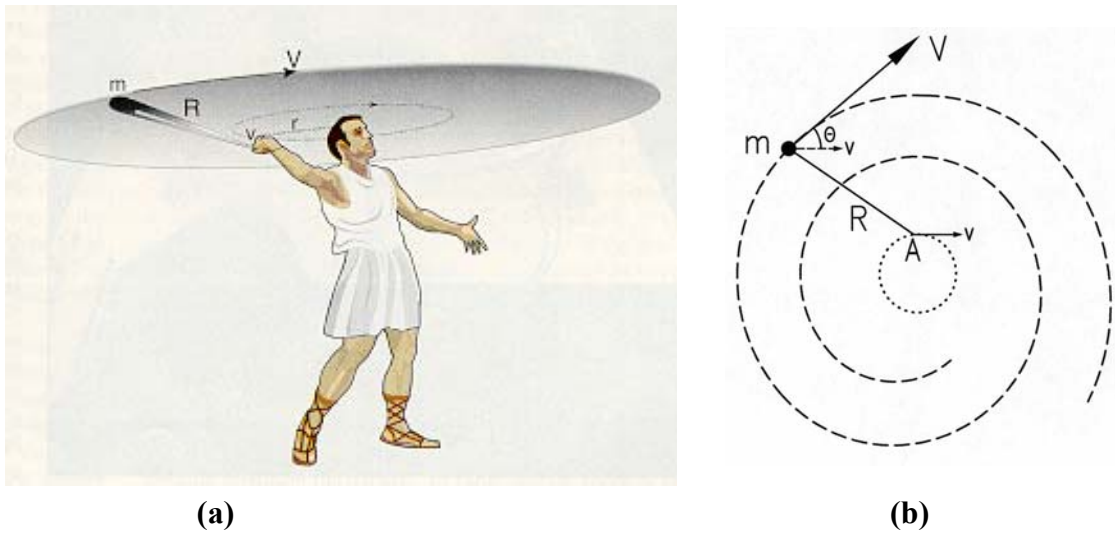


Figure 1.1 Two versions of a classical sling in which the input power $\cong (mV^2 / R)v \sin \theta$ accelerates a projectile by pulling it with a velocity $v \sin \theta$ in the direction of the centripetal force acting on the projectile. Case (a) accelerates a mass by whirling it around with increasing frequency and constant R , whereas (b) shows a mass accelerated by whirling it with a constant frequency, but with an increasing R .

along a spiral path. In this latter case the projectile gains velocity while the sling is operated with a *constant frequency* as point A is pulled around a small drive circle of constant radius r with constant speed v . For a crude example, point A could consist of a hand-held rod with a long string wound around it so that the string unwinds and lengthens as the mass is whirled around its spiral path.

In these two versions of a classical sling the projectile is constrained to follow a circular or spiral path by a centripetal force that is provided by the tension in the string. The projectile, and the end of the string to which it is attached, orbit with a speed $V \cong vR/r$, where $v = 2\pi rf$ is the speed with which the operator's hand at point A moves, and f cps is the cycling frequency. In case 1(a) high speed is achieved by increasing f with constant R , and in case 1(b) high speed is achieved by increasing R with constant f .

These two versions of a classical sling can be operated in a phase stable manner, i.e., so that the angle θ in Figure 1(b) remains approximately constant. To visualize this, note that if the projectile moves forward too rapidly, then θ decreases and the rate at which work is done on the projectile i.e., $\cong v \sin \theta (mV^2/R)$, decreases. If the projectile falls back because it moves too slowly for the sling's cycling frequency, θ and the power input $v \sin \theta (mV^2/R)$ increase and the projectile returns to its stable phase value of θ .

This suggests that the motion is stable, and analysis shows this to be the case when a damping mechanism such as air drag is also included. However, the projectile can also execute a swing in phase θ about its stable phase, and this can be used to add to the projectile speed at the time it is released.

If a string with an infinite tensile strength was available, one could stably whirl a mass to a velocity $\gg 1$ km/sec. However real strings undergo tensile failure, and this typically limits the projectile's maximum velocity to ~ 1 km/sec depending on the materials and design. Tensile failure of the string will occur due to the string's self-mass, even if the string is a high strength steel cable and the projectile attached at the cable end has zero mass. Very high velocity is not achievable in a classical sling for either case 1(a) or 1(b) in Figure 1, although some gain can be made by tapering the cable cross-section and using materials such as carbon polymer cables that have a higher ratio of (strength/density). The slingatron circumvents this tensile failure limit on classical slings, and makes much higher projectile velocity possible.

1.3 Constant-Frequency Spiral Slingatrons, Phase Locking, and Projectile Acceleration Power

Suppose we replace the spiral path in Figure 1(b) with a spiral tube as in Figure 1.2, and mount the spiral on distributed swing arms (or a platform) so that the entire spiral can be propelled with a constant frequency around a small gyration circle of radius r without changing its orientation. In this case the *centripetal force* provided by the accelerator tube constrains the projectile to move along the tube spiral path. The acceleration process is similar to rolling a ball bearing around in a frying pan in a horizontal plane and gyrating the pan around a small circle in order to accelerate the ball bearing to high speed, except that acceleration can occur for a spiral even though the gyration frequency f and gyration speed v are constant. Because projectiles can be phase locked in advancing through the gyrating spiral (as in the case for a classical sling), projectiles can accelerate through many turns and emerge with an extremely high velocity.

Note also that the impulse per unit length delivered to the track by a phase locked projectile moving out along a spiral is the centripetal force multiplied by the time taken to traverse a unit length, i.e., $(mV^2/R)/V \cong 2\pi mf$, where f is the constant gyration frequency and we used $V \cong 2\pi Rf$. This impulse per unit length is *approximately constant* and can be survived by a tube with a constant wall thickness and support structure, regardless of the increasing speed of the projectile as it accelerates out along its spiral path. The slingatron thus avoids the tensile stress limit of the string in a classical sling and is in principle capable of accelerating projectiles to extremely high velocity.

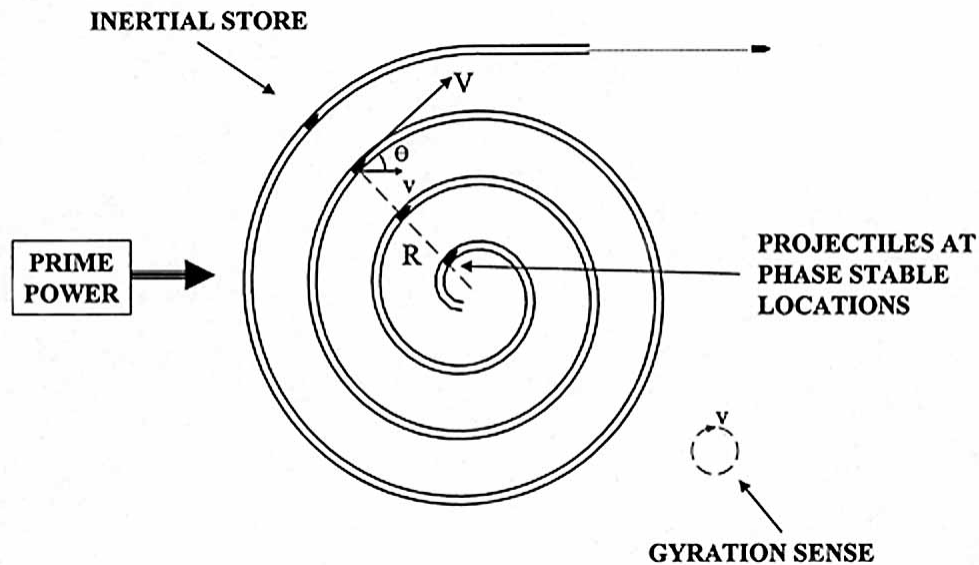


Figure 1.2 A conceptual spiral slingatron in which phase-locked projectiles can be accelerated out through the spiral by the centripetal force provided by the tube as the steel tube continually swings inward at the projectile location. The entire spiral structure swings around a small circle without changing its orientation, i.e., it orbits with constant frequency but does not spin.

Suppose next that one simply anchors a projectile in the spiral tube at its entrance, so that the projectile orbits with the orbiting tube and has a zero speed relative to the tube. Suppose also that the projectile is released when the gyration velocity v is in the half cycle for which its centripetal acceleration has a forward component along the tube and the projectile presses back against the breechblock. After its release, the projectile continues moving with the breechblock until the swing velocity v becomes parallel to the tube ($\theta = 0$). The tube then continues around its gyration circle, but pulls back so that the projectile moves forward relative to the breechblock and starts its acceleration around the first turn. The projectile will then undergo a few phase oscillations that damp via sliding friction, and then lock into to a stable phase θ for continued acceleration through the spiral. This behavior has been confirmed by analysis and computer models, and

occurs provided the radius of curvature of the first spiral turn is no more than a few times the orbiting swing radius r .

Finally we note that neglecting sliding friction, the projectile acceleration power is $(mV^2 / R)v \sin \theta \cong 2\pi fmVv \sin \theta$ where v is the swing speed. For example a projectile of mass 10 kg accelerating in a slingatron that has a swing frequency of 60 cps, a swing speed 150 m/sec, and phase $\sin \theta = 0.5$ consumes a power $283V_{km/s}$ MWatts. This power input to the projectile is extracted from the inertial kinetic energy stored in the orbiting spiral and its attendant structure as the projectile traverses the spiral path. It does not require a separate electrical pulsed power train. The slingatron's inertial energy can be continually replenished between shots using conventional drive motors to maintain the orbiting motion of the system.

1.4 Phase Stable and Phase Swing Motion of a Projectile in a Spiral Slingatron

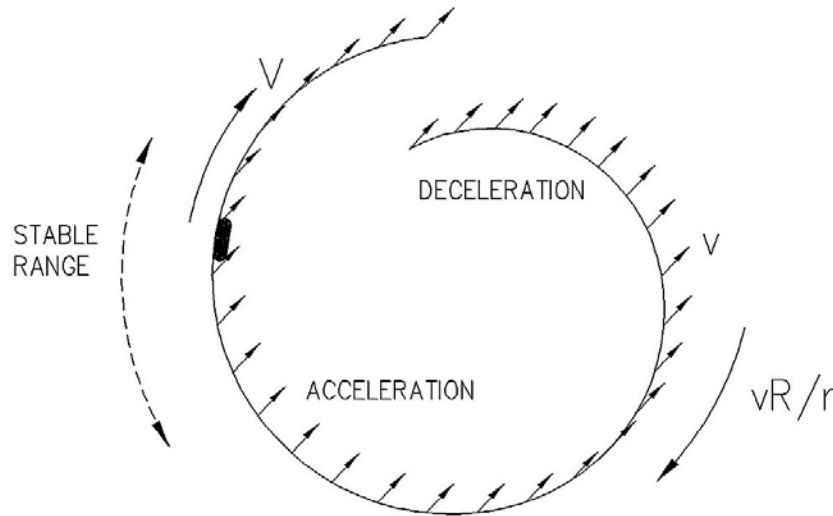


Figure 1.3 A projectile accelerates along a spiral path that gyrates with constant frequency $f = v/2\pi r$. All points of the spiral move in small circles similar to a mixed transverse and longitudinal wave traveling around the track with speed vR/r , and the projectile accelerates on the wave front as the wave speed increases with increasing R .

Figure 1.3 shows a snapshot of a section of the spiral in Fig. 1.2 with the projectile located in a stable phase location of a centripetal wave that travels along the spiral path with speed vR/r . A projectile moving along the track is accelerated if it is located in a region where the track is moving substantially inward along its local radius of curvature, i.e., along the direction of the centripetal force, and the projectile will decelerate if it is located in a section of the track where the track motion is in the opposite direction to the centripetal force. Note that the gyration has a constant frequency so that the track displacement wave speed vR/r is larger in regions where the track radius of curvature R is larger. The projectile can be phase stable in this accelerating wave, as can be seen by

noting that if it moves towards the wave front it will experience a weaker accelerating force and fall back, and if it falls back relative to the wave speed it will experience a stronger accelerating force and move forward relative to the wave. Computer simulations of the motion based on exact equations verify this acceleration, and also its stability if there is some sliding friction to damp phase oscillations. However, it should be noted that it is sometimes advantageous to maximize the exit speed of the projectile by choosing the initial conditions so that the projectile makes a large-amplitude swing in phase before exit, as will be discussed in Chapter 2, i.e., a phase swing is sometimes useful.

1.5 “Soft Collision” View of the Slingatron Acceleration Process

Fig 1.4 shows an imaginary spiral path that is cut into two halves and propelled (instead of gyrated) so that it undergoes a linear oscillation. This oscillation is timed so that when the projectile crosses the cut the spiral instantaneously reverses its constant velocity v so that each successive half always makes a head-on collision with the projectile. Neglecting sliding friction, the projectile then undergoes a series of head-on elastic collisions in which it gains a velocity increment $2v$ each time it crosses the cut, i.e., the gain is $4v$ per cycle. This compares with the larger gain of $2\pi v < \sin \theta >$ per cycle for a phase-locked projectile that travels out along a spiral that gyrates with orbiting speed v . Figure 1.4 provides a more familiar example in which a projectile, in principle, could be accelerated to very high velocity.

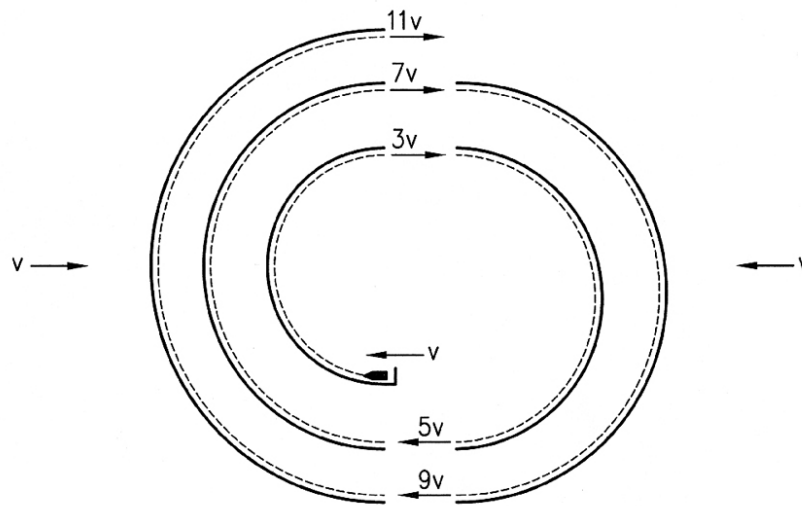


Figure 1.4 An imaginary case in which a spiral undergoes a linear oscillation with constant speed v , with the speed instantaneously reversing each time the projectile crosses the vertical cut so that the projectile experiences a series of head-on collisions with semicircular segments of the spiral.

Note that if the projectile is anchored in front of the blocked breech, as shown in Fig 1.4, and if the projectile is released when the breechblock is moving to the left, then the projectile starts out with a speed v in the laboratory frame and collides with the first track semicircle when the track velocity reverses and moves to the right with velocity v .

Thereafter it continues to accelerate through the system. A similar initial speed can be provided by the breechblock in the case of a gyrating spiral, although a higher injection speed is sometimes desirable for reasons that will be discussed.

1.6 Circular, Spiral, and Hybrid Slingatrons of Reduced Size

In reference 1 we show that a projectile can also gain energy by passing through a gyrating multi-turn ring instead of a spiral tube. However, in this case the projectile undergoes a single large-amplitude swing in phase θ before emerging with a speed that is a multiple of the injection speed. This can be combined with a phase-locked spiral section of tube that serves to accelerate and inject the projectile into a multi-turn ring, as in Fig. 1.5. The purpose of such a hybrid design is that it can result in a projectile being accelerated up to a desired speed V with a slingatron outer radius that is smaller than what would be required to obtain the same final speed using phase-locked spiral acceleration.

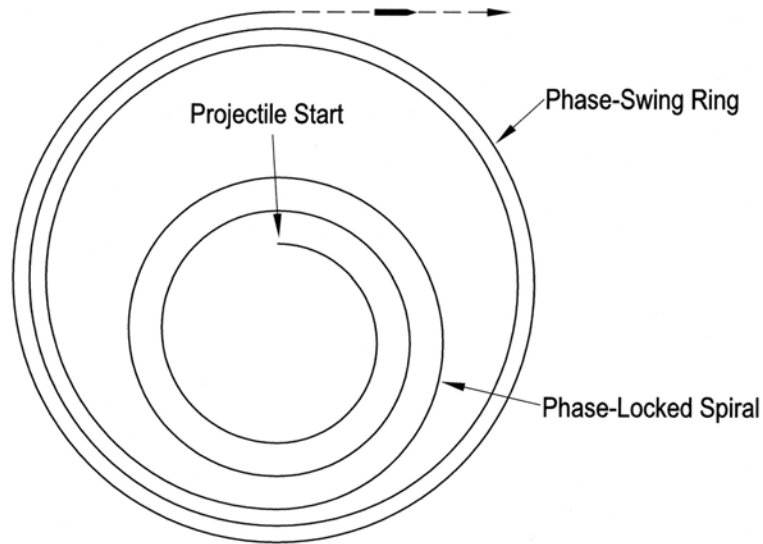


Figure 1.5 A hybrid geometry in which a projectile accelerated in a phase-locked spiral continues on into a phase-swing section consisting of a few turns around a circular path, to achieve a high projectile velocity with an outer radius smaller than given by a simple spiral accelerator.

1.7 The Slingatron as an Inertial Storage System

Off-the-shelf drive motors (combustion or electric) can be used to power the gyration motion of the sling tube. This orbiting motion of the accelerator tube and its attendant structure such as swing arms, bearings, and counterweights, provides an *inertial kinetic energy store*. A projectile accelerating through the spiral tube draws on this inertial energy in its short traversal time through the spiral. A stream of projectiles can also be accelerated through the sling, and the system fire rate would then be determined by the average power available from the drive motors as needed to replenish the swing kinetic energy store between shots. If needed, additional inertial energy could also be stored in

flywheels associated with the swing arm shafts, and these could spin with a substantially higher rim speed than the slingatron tube swing speed. The issues of system mass and size will be discussed in chapters 4 and 5.

1.8 Approximate Equation of Motion for Phase-Locked Acceleration of a Projectile through a Phase Locked Spiral

An approximate equation of motion for the projectile in a slingatron can be obtained by equating the approximate rate of kinetic energy gain for the projectile, $(\partial/\partial t)(0.5mV^2)$, to the power used by the track to displace the projectile in the direction of the centripetal force, $(mV^2/R)v\sin\theta$, minus the power dissipated by the projectile sliding friction, $\mu mV^3/R$, so that

$$m\dot{V} \cong (mV^2/R)(vV^{-1}\sin\theta - \mu) \quad (1.1)$$

Although this equation neglects small terms that are second order in the relatively small quantities v , r , \dot{m} , and μ , it is nonetheless useful for obtaining *estimates* for acceleration in a spiral, assuming a fixed phase-locked value for θ . Exact equations are discussed in the Chapter 2 and are shown to reduce to the approximate equation (1.1) when terms that are second-order in the above small quantities are neglected.

Equation (1.1) shows that (neglecting friction) the accelerating force on a projectile is proportional to the projectile mass, and the acceleration is equivalent to sliding down a small-angle low-friction incline in a large gravitational field of increasing strength V^2/R and decreasing slope angle $\sim vV^{-1}\sin\theta$ where V and v are the projectile and swing velocities and R the local radius of curvature of the sling tube. The accelerating force experienced by a projectile is also distributed along its entire length.

It follows from (1.1) that if the projectile sliding friction is small and the projectile advances out along a spiral path while maintaining a constant relative phase angle θ , the velocity gain per turn ΔV , and gap ΔR between turns, for the case $\mu=0$ are approximately

$$\begin{aligned} \Delta V &\approx 2\pi v \sin\theta \\ \Delta R &\approx 2\pi r \sin\theta \end{aligned} \quad (1.2)$$

We see that the projectile velocity gain per turn can be large.

1.9 Reduced Friction of Large Projectiles and the Prospect of Higher Velocity or Smaller System Size for Large Projectiles

We see from (1.1) that for acceleration to occur we require the sliding friction coefficient to be sufficiently small to satisfy

$$\mu < vV^{-1} \sin \theta. \quad (1.3)$$

i.e., it must decrease with increasing projectile velocity. A theoretical model for the gas film friction predicts that μ will decline with both increasing V and with increasing projectile mass. Experimental data for small polycarbonate projectiles up to 5 km/sec also shows the friction coefficient to decrease with increasing velocity. A high-speed projectile that has a low thermal conductivity bearing side will generate heat that it cannot dispose of except by evaporating its contact surface. This results in a hot gas film on which the projectile slides with a small friction coefficient. A theoretical model for the projectile gas bearing predicts a friction coefficient $\mu(m_{proj}, V)$ that decreases with both increasing projectile speed and size. This occurs because the evaporation-supplied gas film is thicker for larger projectiles, and this reduces the viscous gas shear drag between the underside surface of the projectile and the track. It then follows from (1.3) that projectiles of large mass can be accelerated to higher velocity than small projectiles.

A second consequence of the predicted low friction of large projectiles is that for a large projectile one might choose a smaller value for the swing speed while holding the swing gees, $g_v = v^2 / r$, constant. Note that a smaller swing speed translates into a smaller swing radius, and for a phase-locked spiral the outer radius R required for a final velocity V is given roughly by $R \cong Vr / v = V(\sqrt{r} / g_v)$ so that the system size could be reduced.

1.10 Small-Scale Experimental Demonstration of Projectile Phase Locking

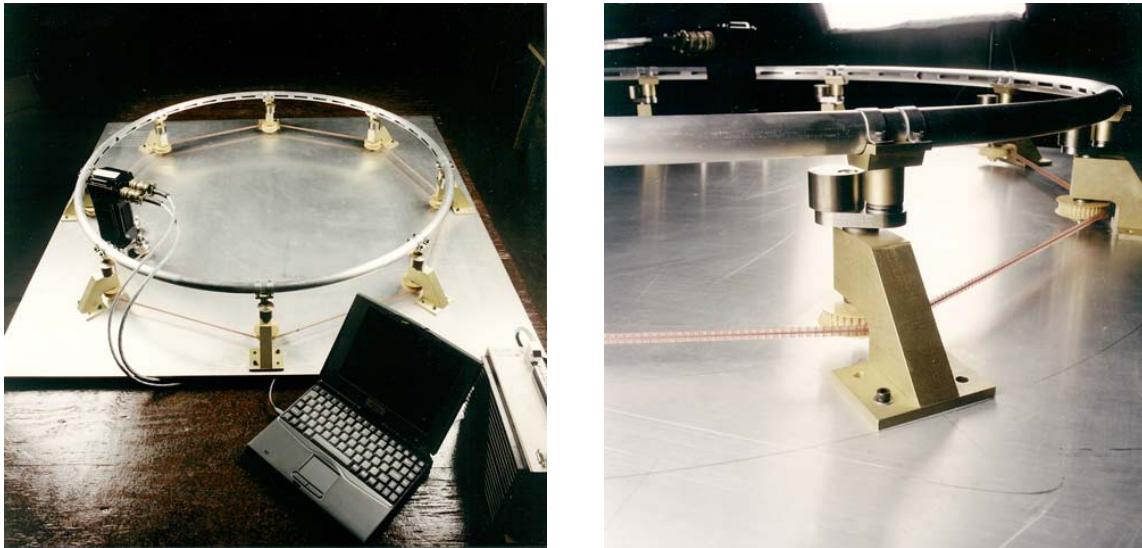


Figure 1.6 This test ring was built in 1995 and had a diameter $2R = 1$ meter. It was mounted on swing arms that gyrated the ring around a swing circle of radius $r = 1.56$ cm at up to $v = 3.1$ m/sec. The machine accelerated ball bearings to $V = 100$ m/s and demonstrated phase-locked acceleration and deceleration.

A small gyrating ring was constructed in 1995 in which ball bearing projectiles could be accelerated, Fig 1.6, and this experiment confirmed the phase-stability of a ball bearing rolling around the ring. The ring could be operated with a steady state gyration, or alternatively could be ramped up in frequency, and in both cases a ball bearing projectile would remain phase-locked with the gyration frequency. The maximum gyration frequency of this low-cost tabletop machine was limited to 32 cps by the available electric motor power and the swing arm structure, and these factors also limited the speed of the rolling ball bearing to 100 m/sec. The maximum speed v of the ring around its gyration circle was 3.1 m/sec and the swing radius $r = 1.56$ cm. The APS Handbook gives the coefficient of rolling friction, $\mu_{roll} = k / r_{ball}$, where the roller radius r_{ball} is in inches, and for a hard steel ball rolling on a steel surface k ranges from 0.0004 to 0.005. Note that rolling friction also becomes smaller as the ball radius increases. However, a rolling projectile cannot be accelerated to hypervelocity since it would deform between 1 and 2 km/sec, whereas sliding projectiles can achieve much higher velocity.

1.11 Angular Dispersion of Projectiles Exiting a Slingatron

We first note that all long-range missions need guided “smart” projectiles regardless of whether they are slings or guns. However, it is worth examining the question of the angular dispersion of slingatron-launched projectiles for shorter-range applications.

One can minimize dispersion by timing the projectile's arrival at the tube exit so that it occurs when the straight section of tube at the exit Fig 1.2 is swinging forward, i.e., parallel to the tube axis. In this case, neglecting vibrations, the projectile has zero transverse kick. This timing could be done passively by choosing the straight section of exit tube to have the correct length, i.e., so that in traversing it the projectile exits when the swing phase of the gyration is such that the tube is moving forward. Alternatively, one might accomplish more precise timing by arranging for the projectile to be slightly early on its approach to the exit. Sensors could then determine the needed correction and switch on a magnetic drag section designed to implement a small slowdown of the projectile to more precisely exit when the tube is moving forward.

It is unlikely that a slingatron could reduce the angular dispersion down to that of a gun designed for precise aiming. However, all mass launchers, including guns and slingatrons, require guided projectiles when used for long-range missions. The slingatron's potential for launch of a large mass to hypervelocity, rapid fire, scalability of the slingatron mechanics to large size, and prime power from conventional motors, make it an attractive candidate for some applications as discussed in Chapter 5.

1.12 Tube Lifetime

The slingatron tube would usually be chosen to be a smooth steel tube. In chapter 3 we include data from some experiments in which high velocity lexan projectiles were fired through a curved steel tube with speeds up to 5 km/sec (using a 2-stage light gas gun) for

the purpose of measuring the sliding friction coefficient of projectiles over a range of velocities. Typically the tube was 1030 drawn-over-mandril steel tube so that prior to its use the tube's inner surface had axially running ridges of typical height about 1.5 microns. After 10's of shots we would cut the tube into segments and examine the surface under a microscope. The surface in these friction experiments showed a slight reduction in the asperity heights (i.e., smoothing) with zero gouging observed.

Note also that a slingatron tube is longer than a conventional gun tube. To minimize the accumulation of snowplowed air and particulates in front of a projectile, designs should provide for vent holes distributed along the tube.

Conventional gun tubes have extremely long lifetimes, whereas EM rail gun tubes have a very short lifetime. The above preliminary data and the fact that the slingatron tube is a steel tube as in a conventional gun, indicate that the lifetime of a steel slingatron tube is expected to be comparable to that of a conventional gun. Note also that some of the shortening of the life of conventional steel gun tubes derives from gas wash with embedded burning particulates flowing into the barrel entrance from the chamber, and this would not occur in a slingatron.

Chapter 3 contains a theoretical model for the projectile sliding friction coefficient and thermal heat diffusion into the steel track from the projectile's hot gas bearing. The short time exposure of the track swept by the hot bearing of a passing projectile, together with the thicker gas film for large projectiles, indicate that the steel track is expected to survive for many shots, as was seen experimentally for small polycarbonate projectiles up to 5 km/sec.

1.13 Estimate of System Mass

The mass M_{system} of a slingatron that accelerates projectiles of mass m_p to velocity V depends on the specific design and materials used plus the slingatron tube swing speed v . Nonetheless we can make some assumptions to obtain a *very rough* estimate for M_{system} for the range $V \gg v$.

First note that a projectile typically accelerates through the slingatron in several gyration periods and emerges with a kinetic energy $0.5mV^2$ that has been extracted from stored inertial energy in the system. Inertial energy is assumed to be stored in two components of the slingatron. The first consists of the orbiting acceleration tube plus its swing arms, outer bearings, and counterweights, that have a total mass m_{swing} and orbiting speed $\sim v$.

The second reservoir of inertial energy is in flywheels that can be located on a subset of the swing arm shafts. These axially symmetric flywheels are assumed to have a rim speed $\sim 3v$, i.e., higher than the gyration speed v of the accelerator ring or spiral tube and its components. We will also assume that the total mass of the flywheels equals m_{swing} , so that the total stored KE in swing tube system plus flywheels is $5m_{\text{swing}}v^2$. This inertial energy stored in the system must provide at least 10 times the projectile's final energy, so

that the gyrating system does not slow down much during transit of a projectile through the slingatron. Equating the stored KE to 10 times the projectile's final KE then gives $m_{swing} \approx m(V/v)^2$. If we also assume that the total system mass comprising the frame, drive motors, flywheels and swing arm units, etc, is 3 times the mass of the inertial energy storage components (swing arms plus acceleration tube structure plus flywheels), we obtain a very rough estimate

$$M_{system} \sim 6m \left(\frac{V}{v} \right)^2 \quad (1.4)$$

We see that the system mass becomes large for high V , but might be reduced if we can implement a larger value for the swing speed v . For example, to launch a projectile of mass m to 2.5 km/sec with a swing speed of 100 m/sec, the system mass estimate is $3.8 \times 10^3 m$. For a higher velocity example, and assuming a swing speed of 400 m/sec, it would take a system mass of $\sim 3750m$ to launch a mass m to 10 km/sec. This second "high-tech" example would require the swing components to orbit in a vacuum or helium environment for example, and the above system mass estimate is probably underestimated. However, it appears possible using advanced fiber Kevlar swing arms etc. The launch rate for these systems for constant-shot-frequency operation would depend on the power of the drive motor assembly needed to replenish the extracted inertial energy per launch.

1.14 Projectile Accelerating Force in Slingatrons compared with Guns

Conventional powder guns and two-stage light gas guns are highly successful mature technologies, and it is interesting to make some comparisons with the potential hypervelocity sling machine discussed here. In a slingatron the accelerating force F in equation (1.1) is *distributed* along the projectile length L and is equivalent to the projectile sliding down a hill in a strong gravitational field of strength V^2 / Rg_E gees and slope $vV^{-1} \sin \theta$. For an estimate of the accelerating force we neglect the sliding friction term in Eq 1.1 and assume that the projectile is phase stable, i.e., θ is constant as it accelerates along its spiral path. Thus as R increases, the projectile speed $V \cong v(R/r)$ also increases in proportion. The propulsion force F from the first term in (1.1) can then be written

$$F(slingatron) = A_{\perp} \left(\frac{L}{r} \right) \rho_{proj} v^2 \sin \theta = mg_v \sin \theta \quad (1.5)$$

where m is the projectile mass and $g_v = v^2 / r$ is the swing acceleration acting on the cylindrical projectile, r and v are the gyration swing radius and swing speed of the spiral tube, $A_{\perp} = \pi D^2 / 4$ is the base cross-sectional area of the cylindrical projectile, and ρ_{proj} is the projectile's average mass density. Note that the propulsion force in (1.5) becomes

larger for projectiles of greater mass, e.g., for increasing length L if D is constant. An example of a large L/D projectile is described in the next section.

Note also that the projectile propulsion force (1.5) in a slingatron is also *independent* of the projectile speed V , i.e., it does not fall off with increasing projectile speed. Thus the power input to the projectile, VF , *increases* with projectile speed, so that extremely high speed could be reached provided the sliding friction coefficient is sufficiently small.

In a conventional powder or gas gun, the projectile accelerating force F_{gun} is due to the gas pressure on the projectile base, i.e., $F(gun) = A_{\perp} P_{base}$. As the projectile speed becomes larger than the gas sound speed, the projectile's base pressure P_{base} in a gun decreases exponentially. There is also a limit to how much one can increase the gas sound speed by increasing the gas temperature and pressure in a gun, since this increases melting and evaporation of the interior surface at the barrel entrance. A large area sabot is also needed for acceleration of very long projectiles in a gun. Within these limits guns are an extremely successful technology, are compact, and have long lifetime steel barrels.

In an EM railgun magnetic field pressure propels the projectile, and is generated by current that flows up one rail, through an armature at the base of the projectile, and back down the other rail. This current becomes detached from the projectile armature at a velocity above a few km/sec and flows through trailing plasma behind the projectile. This presently limits the attainable projectile speed and causes short barrel lifetimes for these research machines, but this problem might be solved in the future.

Although the propulsive force in a slingatron is distributed *along* a projectile, one can nonetheless ask what gas pressure $P(equivalent)$ applied at the projectile base would equal the slingatron propulsive force in (1.5). This equivalent pressure is a constant independent of projectile speed and is given by

$$P(equivalent) = \left(\frac{L}{r} \right) \rho_{proj} v^2 \sin \theta \quad (1.7)$$

For example, a projectile of density 6 gm/cc accelerated in a slingatron with a swing speed of 200 m/sec and average phase angle $\theta = 45^\circ$ would accelerate as if it had an equivalent base pressure of $1.7(L/r)$ kilobars, i.e., typically in the several kilobar range. In section 1.16 we will see that projectiles of very large length/diameter ratio L/D can be accelerated in a slingatron.

1.15 Scaling of Slingatron Mechanics to Geometrically-Similar Machines

Suppose we have designed a slingatron that is mechanically sound. Also, suppose we then fabricate a *geometrically similar design*, i.e., a design for which all spatial dimensions of the original machine have been multiplied by a number β , and operate the

new design with the same gyration swing speed v and projectile exit speed V as the original design. The new design is then also sound, i.e., it appears that one could scale up to fabricate huge versions of these machines.

The size scaling for some quantities are listed below:

PARAMETER	MULTIPLIER
Swing speed v and projectile speed V are constant -----	-1
All spatial dimensions, e.g., swing radius r , tube id, and tube radius of curvature R , and projectile length and diameter L , D , etc -----	β
System mass and its all component masses including projectile mass, etc -----	β^3
Side area and Rated Loads of all bearings -----	β^2
Gyration rpm and max rpm of bearings-----	β^{-1}
Centripetal acceleration at end of swing arms = v^2 / r -----	β^{-1}
Mass carried by bearings at each arm end -----	β^3
Centripetal Force load and bearings Rated Load at swing arm end -----	β^2
Cross section area of each swing arm -----	β^2
Tensile force limit of each swing arm -----	β^2
Gas Bearing Pressure of Projectile $\sim mV^2 / RA$ -----	1
Tube mass per unit length -----	β^2
Projectile impulse delivered to tube per unit length, mV / R -----	β^2
Ratio (Projectile impulse per unit length)/(Tube mass per unit length) -----	1

Based on a theoretical model, projectile sliding friction appears to become smaller for larger projectiles. This is because the projectile gas bearing becomes thicker and its viscous drag per unit area (between the projectile and track surfaces) becomes smaller. This would allow higher projectile velocity to be obtained by larger projectiles and machines. Some preliminary scaling based on a simple theoretical model gives:

Projectile sliding friction (see unpublished note)-----	$\sim \beta^{-1/2}$
Projectile fractional mass loss at exit -----	$\sim \beta^{-1/2}$
Temperature increase of the steel slingatron track immediately after traversal by a projectile is the same for various sizes. -----	1

1.16 Slingatron Projectiles of Large Mass and (Length/Diameter) Ratio and Comments on Atmospheric Traversal

Although there appear to be many potential applications for slingatrons, we will give only one example here, assuming that this conceptual mass accelerator works properly. From the above scaling laws it appears that projectiles of very large mass could be accelerated,

and they could have both a large (Length/Diameter) ratio, e.g., ~ 50 , as well as a large mass, e.g., ~ 1 ton. Such projectiles would be capable of traversing the earth's atmosphere with negligible velocity loss from atmospheric drag. A slingatron thus appears to have the potential to launch streams of high velocity projectiles to deliver materials to remote destinations around the globe or into space for commercial transport.

and they could have both a large (Length/Diameter) ratio, e.g., ~ 50 , as well as a large mass, e.g., ~ 1 ton. Such projectiles would be capable of traversing the earth's atmosphere with negligible velocity loss from atmospheric drag. A slingatron thus appears to have the potential to launch streams of high velocity projectiles to deliver materials to remote destinations around the globe or into space for commercial transport.

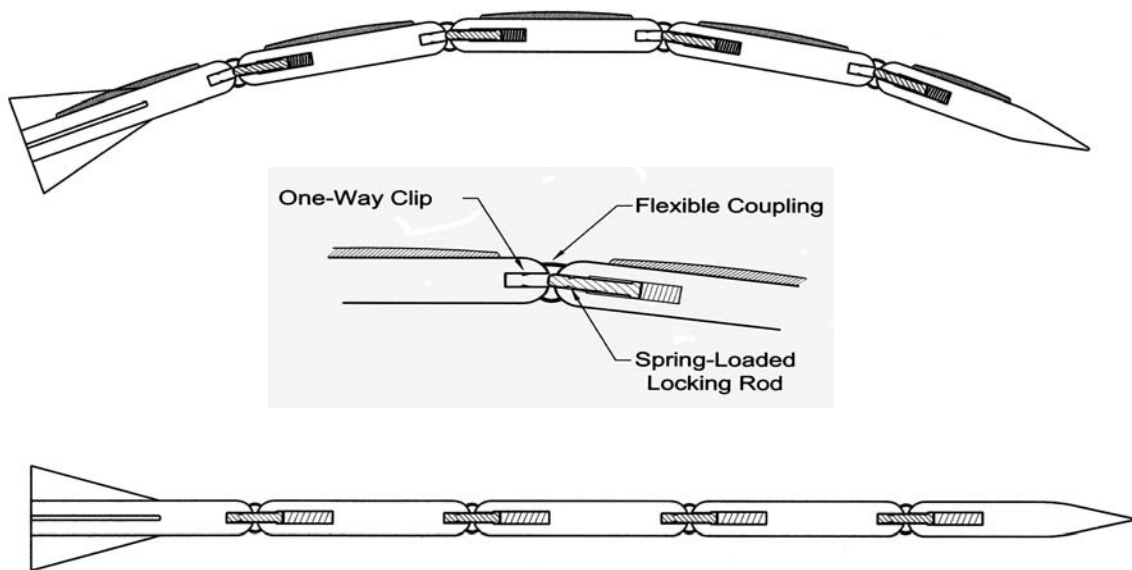


Figure 1.7 A large L/D projectiles with rigid segments and flexible connections can conform to a curved track for acceleration in a spiral slingatron. At exit the projectile traverses a straight section of tube in which alignment of the segments allows spring-loaded locking rods to be driven into neighboring segments to lock the projectile into a straight condition.

Note that because the L/D ratio is large, the projectile load would be shared by a large segment of the machine. This potential appears to exist due to the favorable scaling of the mechanics of slingatrons to large size.

Figure 1.7 shows a projectile design concept in which an elongated projectile consists of segments that allow it to conform to the changing curvature of the slingatron tube along its path through the accelerator. It also has a layer of material that evaporates to supply the gas bearing on its track side. On approach to the exit the projectile passes through a

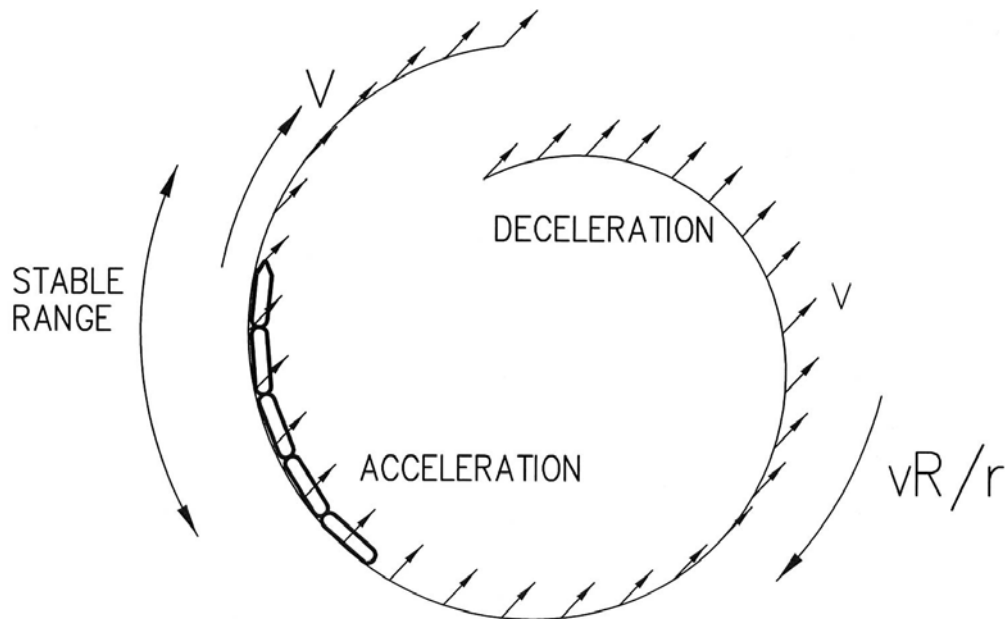


Figure 1.8. A large L/D projectile shown in an inner turn of a spiral slingatron when the gyration velocity v of the spiral assembly is as shown by the small arrows. The projectile is trapped in the accelerating wave that advances with speed vR/r as the gyration velocity vector rotates.

short straight section that causes alignment of the segments, and this in turn allows spring-loaded locking rods to be driven into their neighboring segments so that the projectile becomes locked into a rigid straight condition. Tail fins would also be deployed for flight through the atmosphere, and residual bearing material would be burnt off in the atmosphere. Elongated projectiles could be stored in some inner turns that function as a storage magazine that is a part of the gyrating platform as discussed in Chapter 4.

Figure 1.8 shows a projectile on which work is done as the track swings inward with a velocity component in the direction of the centripetal force acting on the projectile. The accelerating force is distributed along the projectile length and is proportional to the distributed projectile mass. An imaginary observer riding on the projectile would experience the trip as sliding downhill in a gravitational field.

Consider a simple idealized example in which such a projectile is launched from sea level with velocity V_o and an elevation angle ϕ with the horizontal. For estimates we neglect loss due to earth's gravity and estimate only the velocity loss due to air drag in traversing the earth's atmosphere. We assume an exponential atmosphere of scale height $h = 8$ km and a sea-level air density $\rho_{air} = 1.2 \times 10^{-3} \text{ gm/cc}$. After obliquely traversing the entire atmosphere at an elevation angle ϕ , the projectile velocity loss ΔV due to atmospheric drag would then be given by

$$\frac{\Delta V}{V(0)} = \frac{V(0) - V(\infty)}{V(0)} = \left\{ 1 - \exp\left(-\frac{C_D \rho_{air} h}{2L \rho_{proj} \sin \phi}\right) \right\}$$

We assume that the projectile approximates a cylinder of length L , diameter d , and density ρ_{proj} , so that its mass m is

$$m \cong \frac{\pi}{4} d^3 \left(\frac{L}{d}\right) \rho_{proj}$$

For example, choosing $m = 10^6 \text{ gm} = 1 \text{ ton}$, $L/d = 50$, $\rho_{proj} = 4 \text{ gm/cc}$, the projectile diameter follows as $d = 18.5 \text{ cm}$ and length $L = 927 \text{ cm}$. Assuming the projectile drag coefficient is $C_D = 0.1$, and the launch elevation angle $\phi = 30^\circ$, the percentage velocity loss of the projectile due to air drag for this oblique pass through the atmosphere would be $\cong 2.6\%$.

We see that such projectiles would experience only a small velocity loss due to atmospheric drag, and could be launched obliquely through the atmosphere to various locations around the globe. They could alternatively be inserted into LEO using a small velocity kick at apogee. Such projectiles would traverse the atmosphere in a brief few seconds at the launch and re-entry ends, so that although some ablation would occur in the nose region, heat would only have time to diffusively advance a short distance into the side surface of the projectile, i.e., projectiles would arrive at their destinations without major thermal damage. Ablative out-blowing from the hot projectile surface also provides a shielding factor that reduces heat transport into a projectile.

APPENDIX

Recovery of Equation (1.1) from Exact Equations

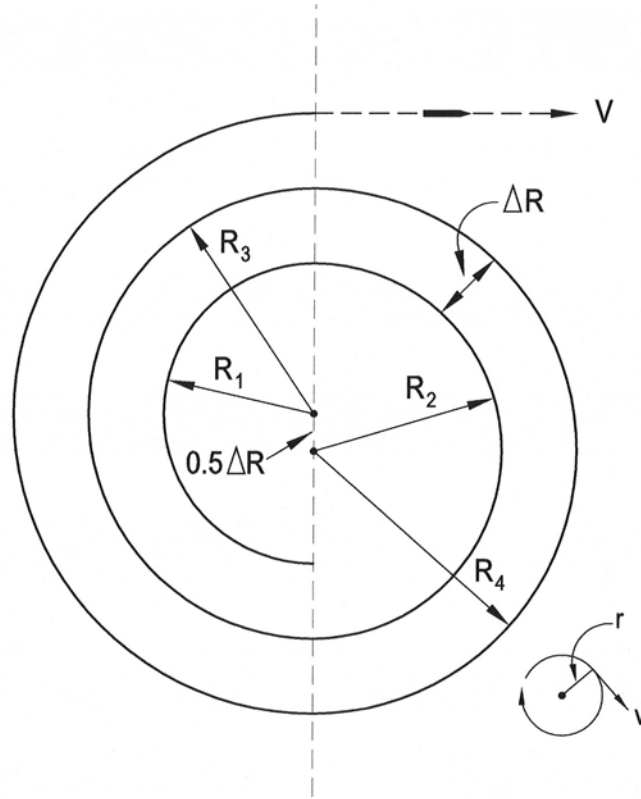


Figure A1. Spiral of connected semicircles with radii $R_n = R_1 + 0.5(n-1)\Delta R$

Here we give a more accurate analysis for a spiral slingatron in which the accelerator tube is configured as a series of semicircles as in Fig. A1. Construction of a spiral from a series of semicircles simplifies the equations and also some aspects of the fabrication of such a device. Figure A1 shows an example in which the semicircles have radii R_n , with centers alternately located at two points spaced by $0.5\Delta R$ so that the gap between turns is ΔR . The semicircles connect on a diameter as shown so there is no discontinuity in projectile speed or direction in crossing from one semicircle to the next, but there is a jerk as the centripetal acceleration of the projectile changes from V^2/R_n to V^2/R^{n+1} . The entire spiral orbits around a circle of radius r in the laboratory frame without changing its orientation. Its gyration frequency is constant, and the spiral gyration and projectile motions are in the clockwise direction.

Figure A2 shows a projectile of mass m sliding with speed V along a segment of the track shown in Fig A1, for which the radius of curvature R is constant. We include sliding friction in the equations of motion, but will not include the projectile mass loss due to

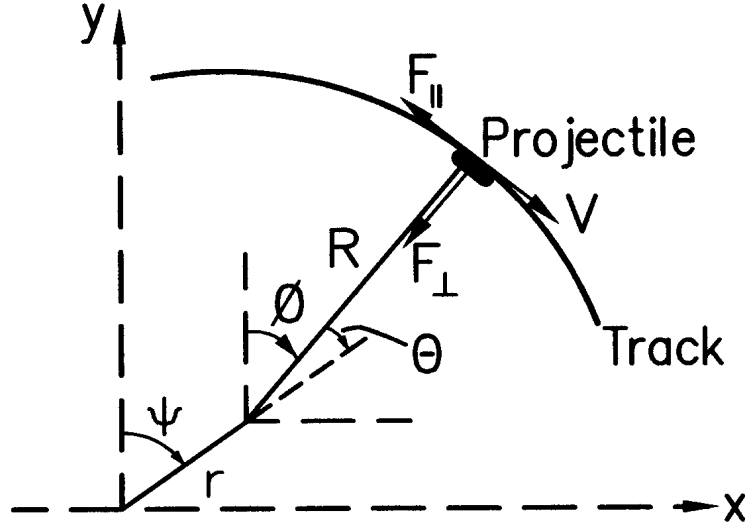


Figure A2 A semicircular section of a spiral track that swings around a gyration circle of radius r with constant speed $v = r\dot{\psi}$ without changing its orientation.

evaporation of its contact surface into the gas bearing. The equations of motion for the projectile located at (x, y) are then,

$$\begin{aligned}
 m\ddot{x} &= -F_{\perp} \sin \phi - F_{\parallel} \cos \phi \\
 m\ddot{y} &= -F_{\perp} \cos \phi + F_{\parallel} \sin \phi \\
 F_{\parallel} &= \mu F_{\perp}
 \end{aligned} \tag{A1}$$

where m is the sliding friction coefficient of the projectile. Since the projectile is constrained to move along the track, we also have

$$\begin{aligned}
 x &= r \sin \psi + R \sin \phi \\
 y &= r \cos \psi + R \cos \phi
 \end{aligned} \tag{A2}$$

Combining (A1) and (A2) and noting $\ddot{\psi} = 0$ gives the projectile equation of motion and the relevant velocities,

$$\begin{aligned}
 R\ddot{\phi} - r\dot{\psi}^2 \sin(\psi - \phi) &= -\mu R\dot{\phi}^2 - \mu r\dot{\psi}^2 \cos(\psi - \phi) \\
 V &= R\dot{\phi} \\
 V_{lab} &= (\dot{x}^2 + \dot{y}^2)^{1/2} = \{R^2\dot{\phi}^2 + r^2\dot{\psi}^2 + 2rR\dot{\phi}\dot{\psi} \cos(\psi - \phi)\}^{1/2} \\
 v &= r\dot{\psi} = 2\pi r f
 \end{aligned} \tag{A3}$$

where V and V_{lab} are the speeds of the projectile relative to the track and in the laboratory frame, v is the constant orbiting speed of the entire track in the laboratory frame, and $\mu(m, V)$ is the projectile sliding friction coefficient which is dependent on projectile mass and velocity for a given projectile geometry and choice of materials. The first part of (A3) can be rewritten,

$$\begin{aligned}\dot{V} &= \frac{v^2}{r}(\sin \theta - \mu \cos \theta) - \frac{\mu V^2}{R} \\ \theta &= \psi - \phi\end{aligned}\tag{A4}$$

where θ is the relative phase angle between the velocity vectors \mathbf{v} and \mathbf{V} as shown in Fig A2. Numerical solutions for this equation are given later in this chapter.

Recovery of the Approximate Equation (1.1)

It is useful to note that throughout most of the acceleration μ and v/V are small quantities. This enables us to obtain an *approximate* equation of motion for the projectile obtained by dropping the term $-\mu(v^2/r)\cos \theta$ on the right of (A4), so that

$$\begin{aligned}\dot{V} &\cong \frac{v^2}{r} \sin \theta - \frac{\mu V^2}{R} \\ \theta &= \psi - \phi\end{aligned}\tag{A5}$$

Suppose also that the projectile accelerates along the orbiting spiral with a phase angle θ that is approximately constant, i.e., $\dot{\theta} \cong 0$, so that $V \cong Rv/r$. Equation (A5) then gives

$$\dot{V} \approx \frac{V^2}{R} \left\{ \frac{v}{V} \sin \theta - \mu \right\}\tag{A6}$$

i.e.,

$$\frac{d}{dt} \left(\frac{1}{2} m V^2 \right) \approx \frac{m V^2}{R} \{ v \sin \theta - \mu V \}\tag{A7}$$

We see that (A7) displays approximately the work done on the projectile by pulling it inward with a velocity component $v \sin \theta$ in the direction of the centripetal force, minus the friction drag power as used for the approximate discussion in Chapter 1. These approximations break down if significant swings in the relative phase angle $\theta = \psi - \phi$ occur, or if the friction term becomes significant. However, exact numerical solutions to the more exact equations (A3) and (A4) can easily be obtained. Calculations show that the sliding friction coefficient decreases with increasing projectile speed and mass and this should also be taken into account in numerical models, along with the attendant mass loss of the projectile and track heating.